

# POSITION/FORCE CONTROL OF A 1-DOF SET-UP POWERED BY PNEUMATIC MUSCLES

Aron Pujana-Arrese, Kepa Bastegieta, Anjel Mendizabal, Ramon Prestamero and Joseba Landaluze  
*IKERLAN Research Centre, Arizmendiarrieta 2, E-20500 Arrasate (The Basque Country), Spain*

**Keywords:** Pneumatic muscle, Robotic Arm, Position/Force Control, Hybrid Control, Impedance control.

**Abstract:** A one-degree-of-freedom set-up driven by pneumatic muscles was designed and built in order to research the applicability of pneumatic artificial muscles in industrial applications, especially in wearable robots such as exoskeletons. The experimental set-up is very non-linear and very difficult to control properly. This paper describes the control of this mechatronic system's interaction with its environment, controlling both its position and the force exerted against it. The classic position/force control techniques - hybrid control and impedance control - have been adapted to pneumatic muscles and applied to the experimental set-up developed. An alternative solution is also proposed whereby force or torque control is based on the calculation made by an estimator instead of on direct measurement by a sensor. The article presents a detailed analysis of the force and torque estimator used to close the control loops in the two position/force control schemes. Finally, the article concludes by presenting the experimental results obtained and the most outstanding conclusions of the study as a whole.

## 1 INTRODUCTION

The group of researchers from the IKERLAN technology centre working on the development of mechatronic systems have been involved for the last three years in the design and construction of an upper limb IAD (Intelligent Assist Device) (Martinez, 2007; Martinez, 2008). More specifically, the device is an exoskeleton for helping the user carry out routine tasks in the workplace (Figure 1). One of the requirements established from the start was to include non-conventional actuators as far as possible. Among the alternatives studied, artificial pneumatic muscles were considered to be the most suitable forms of actuation. In order to study the applicability of this type of actuators in biomechatronic systems a 1-DoF experimental set-up was built, driven by a pair of antagonistic pneumatic muscles. Initially, a dynamic model of the pneumatic muscle was created, and then used to make the full model of the experimental set-up. This model was experimentally validated (Pujana-Arrese, 2007).

Motivated by the high degree of non-linearity of the experimental prototype, the authors developed different solutions for robust control of the system's

angular position: from a first initial attempt using basic controllers, to more advanced techniques achieved such as  $H_\infty$  or the non-linear sliding mode technique (Pujana-Arrese, 2008; Arenas, 2008).

This paper takes a step further as regards control of the mechatronic system's interaction with its environment, controlling not only the position but also the force exerted against it. An alternative



Figure 1: Exoskeleton ÍKO (IKerlan's Orthosis) worn by a dummy.

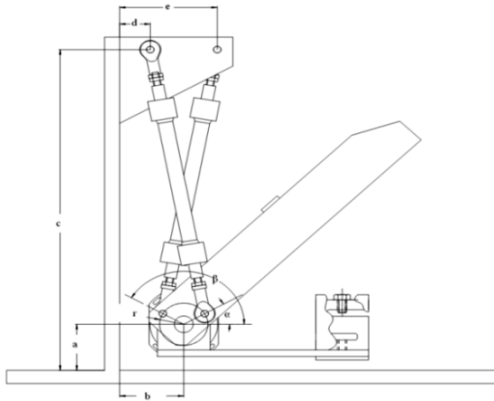


Figure 2: Geometric model of the 1-DoF robotic arm.

solution is also put forward whereby the force or torque control is based on the calculation made by an estimator instead of on direct measurement by a sensor.

A classic, in the field of the position/force control, is the Hybrid Controller strategy put forward by Raibert and Craig (1981). The controller carries out its action using selection matrixes which establish some spatial directions where position control must be carried out and some others where force must be controlled. In this way the force and position control actions are uncoupled by using the appropriate treatment of the spatial geometry where the manipulation task is being carried out. Another classic strategy is Impedance Control (Hogan, 1985), which does not control the position or the force but the dynamic relation between the two. This type of control strategy is deemed to be very suitable for IADs, although it needs to be adapted depending on the specific application.

The object of this paper is to present the algorithms implemented for controlling interaction with the environment, stressing the fact that an estimator requiring no direct measurement of either the torque or the force exerted by the mechatronic device has been developed for this purpose. The first point contains a brief description of the experimental set-up used for this study, and the paper then goes on to present a theoretical review of the control techniques most commonly used for these ends: Hybrid Control and Impedance Control. There then follows an in-depth analysis of the force and torque estimator used to close the control loops in both cases, and there is then a detailed description of the control diagram used for both the Hybrid Control and Impedance Control. Finally, the article concludes by presenting the experimental results obtained, and the most outstanding conclusions of the study as a whole.

## 2 SET-UP DESCRIPTION

A human arm orthosis-type application has been taken into consideration when designing the set-up. To this end and albeit with a single degree of freedom, it was considered that it should allow for the greatest angular displacement possible, and that it should be able to transport the greatest mass possible at the tip (emulating a weight borne by the hand). On the other hand, however, it needed to be confined to the length of the pneumatic muscles. In seeking a compromise between all the specifications, a displacement of around  $60^\circ$  and a maximum mass to be moved at the tip of 8 kg were set. By trying to minimize the length of the muscle required, the design focused on the mechanism that would enable the arm and inertias to rotate with good dynamics by means of the two muscles.

The pneumatic muscle that was chosen was the DMSP-20-200N manufactured by Festo. Figure 2 and Figure 3 show the resultant mechanism and a picture of the prototype. The parameter values that define the mechanism are:

$$a=5 \text{ mm}; b=85 \text{ mm}; c=491 \text{ mm}; d=40.6 \text{ mm} \\ e=129.4 \text{ mm}; \alpha=0^\circ-60^\circ; \beta=120^\circ-180^\circ; r=32 \text{ mm}$$

From these values the distance  $L$  (mm) between the ends (joining points of the mechanism) of the pneumatic muscles is:

$$L = \sqrt{175059 + 2841.6 \cdot \cos \alpha - 26624 \cdot \sin \beta}$$

When the muscles are without pressure, the distance  $L$  is of 423 mm, with the length of the muscle fibre being 200 mm. The centre of the arm mass with regard to the centre of rotation is at a height of 17.6 mm and at a horizontal distance of 205 mm, considering that the arm is in the horizontal position. The arm mass is 0.987 kg. The centre of the additional masses placed on the end of the arm would be at a height of  $-24$  mm and at a horizontal length of 367 mm with regard to the centre of rotation, always bearing in mind that the arm is in the horizontal position. The set-up may be rotated so that the arm moves in a horizontal plane and the effects of gravity are therefore cancelled out. The prototype (Figure 3) includes a *FAGOR S-D90* encoder, which supplies 180,000 pulses per turn, and a load cell on the lower stop of the model.

The schematic diagram of the set-up, which includes the control hardware, sensors and pneumatic circuit, is shown in Figure 4. As the figure shows, two *Festo MPYE-5-1/8HF* pneumatic servo-valve are used for actuation, each linked to

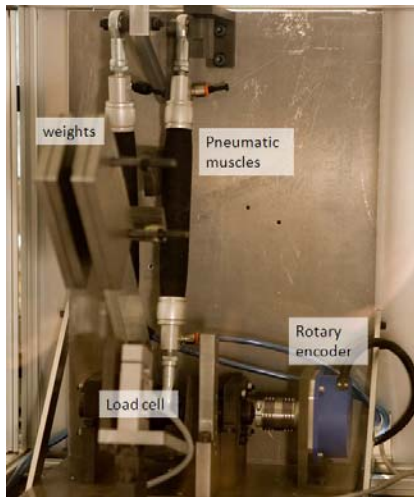


Figure 3: Picture of the experimental set-up.

one pneumatic muscle and controlled independently by the controller. The controller hardware is *PIP8*, an industrial PC made by the company MPL, which is very similar to The MathWorks' *xPCTargetBox*. A PC104 card (*Sensoray model 526*) was incorporated into the *PIP8* in order to read and write all the system signals. Control algorithms were implemented in *Simulink* and code was generated and downloaded in the aforementioned hardware by means of two of The MathWorks' tools: *RTW* and *xPCTarget*.

### 3 POSITION/FORCE CONTROL ALGORITHMS OVERVIEW

Research into pneumatic muscles has been carried out considering them as orthosis actuators. And an orthosis, or exoskeleton, is a wearable robotic device. In an initial approach, the basic control of an orthosis-type device can be considered to be based on position control, where the user creates the movement set-point and closes the loop aided by the human body's own sensors. Detecting the user's *intention* and creating the movement set-point on the basis of this is a key element. Another very important factor to be taken into account is the interaction with the environment, whether from the perspective of controlling the force exerted so as not to cause damage to persons within the robotic device's field of action, or because the device is being used as a force augmentation system. From this point of view, its functioning is similar to that of a robotic manipulator. There are two classic position/force schemes for robotic manipulators:

hybrid control and impedance (or admittance) control. These schemes have been considered valid for the case of an arm orthosis, although they have some special characteristics that must be taken into account when the actuators are pneumatic muscles.

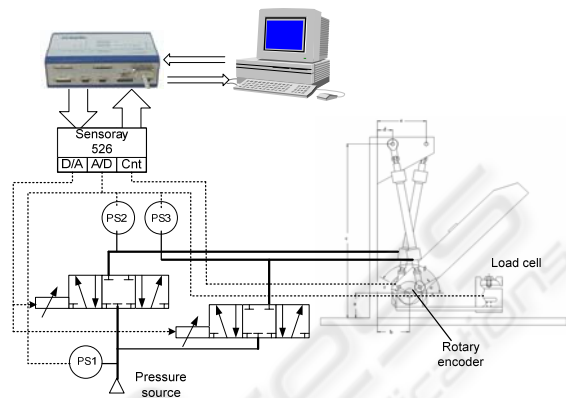


Figure 4: Schematic diagram of the set-up and pneumatic circuit.

#### 3.1 Hybrid Position/Force Control

Hybrid control is a conceptually simple method for controlling both the position and the contact force generated at the tip of a manipulator during a task involving restricted movement. The method does not specify any feedback control law for regulating the errors, but rather a control architecture in which any position and force control techniques can be considered. The principle of hybrid control is based on the idea that each manipulation task can be described by specifying a set of contact surfaces. These surfaces serve to detail the restrictions existing in the system, which may be either *natural* or *artificial*.

The *natural restrictions* are connected with the system's particular mechanical and geometrical characteristics. *Artificial restrictions*, on the other hand, are connected with the control task objectives, and are specified in terms of position or force parameters.

Natural and artificial restrictions are defined within the space of the task, not within the space of the actuations. One natural and one artificial restriction may be specified for each degree of freedom of the task. In general, taking the task geometry into account, it is not difficult to determine the natural restrictions existing and decide on the most suitable way of dividing the space of the task on the basis of these.

For the case of an orthosis, normally *mixed* exercises are performed, which consist of both



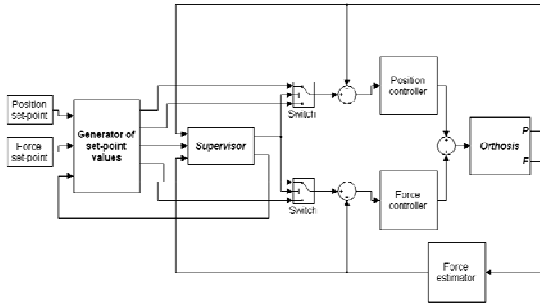


Figure 5: Structure of the hybrid position/force controller.

stages of free movement and stages of restricted movement. The restricted movement part can be of much less importance than in the case of a robotic manipulator, any may simply consist of a force control loop, which does not necessarily have to act at the same time as the position control in other directions. In any case, a *supervisor*, able to switch between the different configurations of the manipulator and the corresponding control laws, is a key element. A supervisor of this type must pay special attention to the impact between the manipulator and the environment, and to its separation.

Figure 5 shows a diagram of position/force hybrid control valid for both an orthosis and the 1-DOF set-up used to analyse the specific case of the pneumatic muscles. It basically consists of two independent controls, one for position and the other for force, and a supervisor that switches between one control type and another depending on the contact with the environment. The supervision is based on the information on the force exerted, which may be provided by a force sensor or an estimator. The supervisor, at the same time as the set-point generator, makes the transition between the controllers in a *soft* manner, to prevent rebounds and to assure the system's stability.

As already mentioned, the hybrid control scheme does not impose the control techniques that are used for the position controller and for the force controller.

### 3.2 Impedance Control

Impedance control is another classic force control scheme, and it is of great interest in the case of orthoses. It does not require a supervisor and it is able to take on the control of a composite task, with free and restricted movement stages, maintaining the system's stability without changing the control algorithm. It is based on the idea of controlling the dynamic relationship between the force and position

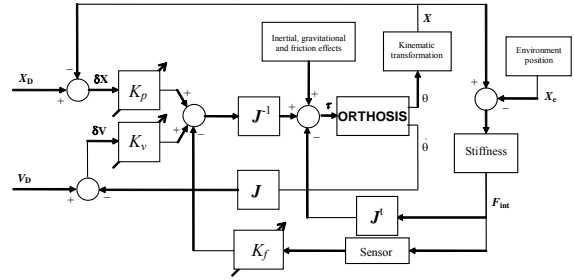


Figure 6: Structure of the impedance controller.

variables of the physical systems. It is presumed that in any manipulation task the environment contains inertias and kinematical restrictions, i.e. systems accepting forces as input and responding by means of displacements (admittances). The manipulator in contact with the environment must accordingly behave as an impedance and respond with a determined force to the displacement of the environment. The general strategy may be established in terms of controlling a movement variable and at the same time providing the manipulator with a disturbance response in the form of impedance. Thus, the interaction between the manipulator and its environment can be modulated and controlled by acting on the impedance values.

In impedance control, the functional form of the torque of a manipulator's actuators is well-known:

$$\begin{aligned} \tau_{act} = & I(\theta)J^{-1}(\theta)M^{-1}K[X_0 - L(\theta)] + S(\theta) \\ & + I(\theta)J^{-1}(\theta)M^{-1}B[V_0 - J^{-1}(\theta)\omega] + V(\omega) \quad (1) \\ & + I(\theta)J^{-1}(\theta)M^{-1}F_{int} - J^t(\theta)F_{int} \\ & + I(\theta)J^{-1}(\theta)G(\theta, \omega) + C(\theta, \omega) \end{aligned}$$

where each line of the second member represents a contribution of a different nature to the total torque. The first line corresponds to terms dependent on the position, the second to terms of speed, the third to terms of force, and the fourth to terms of inertial coupling. Within the field of the actuations, this equation expresses the behaviour that the controller should be able to induce in the manipulator, in the form of a non-linear impedance. The input variables are the desired Cartesian positions and speeds, and the terms – linear or not – that specify the required dynamic behaviour, characterised by the magnitudes  $M$ ,  $B$ , and  $K$ . Figure 6 shows the typical impedance control structure for a robotic manipulator or for an orthosis, in which the feedback gains of the position, speed and force loops,  $K_p$ ,  $K_v$  and  $K_f$  respectively, depend on the reference inertia and mass tensors and on the values designed for stiffness,  $K$ , and damping,  $B$ , and they are deduced from the control law (1).

The force feedback  $F_{int}$ , based on a measured force or estimated force, has the effect of changing the apparent inertia of the manipulator. However, the impedance control scheme can also be applied without a sensor or force estimator. In this case the force is not explicitly controlled, but, depending on the impedance values used in the controller design, the force the system exerts on the environment is limited.

#### 4 TORQUE/FORCE ESTIMATOR

As already mentioned in the introduction, on most occasions different sensors are used to directly measure the force or torque exerted by the actuators in order to control the interaction between the mechatronic system and its environment (Tsagarakis, 2007; Jia-Fan, 2008).

This paper puts forward the idea of carrying out the control of the interaction between a mechatronic system driven by pneumatic muscles and its environment without any direct measurement at all of either the torque exerted by the pneumatic actuators or the force exerted by the arm. The torque and force are calculated on an estimated basis from the angular position of the arm and the pressures on the pair of muscles, as set out in the ensuing paragraphs.

The force exerted by each muscle can be modelled on the basis of its contraction and interior pressure according to equation (2) (Pujana-Arrese, 2007).

$$F_{up/down} = (D_1 + D_2 \cdot q_{up/down} + D_3 \cdot q_{up/down}^2) P_{up/down} + \varphi(q_{up/down}) \quad (2)$$

where

$$\varphi(q) = a + b \cdot q + c \cdot q^2 + d \cdot q^3 + e \cdot q^4 \quad (3)$$

$q$  is the contraction of each muscle (*up* and *down*),  $P$  is the pressure exerted on each muscle, and the parameters  $D_1$ ,  $D_2$ ,  $D_3$ ,  $a$ ,  $b$ ,  $c$ ,  $d$  and  $e$  are constants obtained from empirical tests for characterising the behaviour of the muscles (Pujana-Arrese, 2007).

To calculate muscle contraction, trigonometric formulas are used to relate this contraction with the angle formed between the arm and the vertical (Figure 2). The torque exerted by the combination of the two pneumatic muscles ( $\tau_{pres}$ ) can thus be deduced as:

$$\begin{aligned} \tau_{pres} = & F_{up} \cdot r \cdot \sin\left[\left(\frac{\pi}{2} - (\theta_{top} - \theta)\right) \right. \\ & \left. + \left(\frac{\pi}{2} - \alpha_{up}\right)\right] - F_{down} \cdot r \\ & \cdot \sin\left[\left(\frac{\pi}{2} - (\theta - \theta_{down})\right) \right. \\ & \left. + \left(\frac{\pi}{2} - \alpha_{down}\right)\right] \end{aligned} \quad (4)$$

where  $F_{up}$  is the force exerted by one pneumatic muscle,  $F_{down}$  is the force exerted by the other pneumatic muscle, and  $r$  is the distance between the rotation point and the lower joining points of the pneumatic muscles. The angle of the arm with respect to the vertical is designated as  $\theta$ , while  $\theta_{top}$  and  $\theta_{down}$  are the angles corresponding to the physical limit stops of the prototype.  $\alpha_{up}$  is the angle formed with respect to the horizontal by the muscle designated as *up*, while  $\alpha_{down}$  is the angle formed by the other muscle with respect to the horizontal.

Despite the good results obtained on simulation, the experimental tests showed lack of accuracy of the estimated value with regard to the torque actually exerted by the muscles. The main reason for this is that equation (2) does not contemplate hysteresis, which is a feature of the pneumatic muscles. The error assumed on ignoring the effects of hysteresis means the estimator is not applicable in cases where the arm moves freely. However, when the arm is blocked by collision, the pressures, and consequently the torque, increase in such a way that the measurement error is not critical.

In order to obtain an estimator that behaves correctly for free movement, with the system moving at low torque values, a development based on Newton's laws of motion is proposed. This new estimator calculates the torque by means of equation (5), which is in fact the development of Newton's second law of motion.

$$\tau_{newt} = m \cdot g \cdot L \cdot \sin(\theta - \beta) - N \cdot m_p \cdot g \cdot L_p \cdot \sin(\theta - \beta_p) + \ddot{\theta} \cdot I_o \quad (5)$$

where  $m$  is the mass of the arm,  $L$  the distance between the rotation point and the arm's centre of gravity,  $\theta$  the angle between the arm and the vertical,  $\beta$  the angle between the rotation point and the centre of gravity, and  $I_o$  its inertia on the rotation point.  $N$  is the number of extra masses placed on the tip, and  $m_p$  is the weight of each mass ( $N \cdot m_p$  thus represents the mass placed at the tip of the arm).

This torque estimator functions correctly but has two negative aspects. The first is that if the structure has two or more degrees of freedom instead of one, calculating the equation becomes rather complicated. The other aspect is that if any kind of interaction is produced with the environment, e.g. a collision, when the arm movement is blocked

equation (5) is no longer of use for estimating the torque exerted by the actuators.

Knowing that the torque estimator based on Newton's law of motion calculates the torque correctly in the case of free movement, and that the moment evaluated by the torque estimator based on the muscle pressures can be acceptable when an interaction occurs with the environment, it was decided to create a hybrid torque estimator. This hybrid estimator requires some kind of observer to indicate whether an interaction with the environment has occurred, so that the desired estimator can be selected at each time. In short, when free movements are made the estimator used will be the one based on Newton's laws ( $\tau_{newt}$ ), and in the case of limited movements or interactions with the environment the estimator used will be the one based on the pressures of each muscle ( $\tau_{pres}$ ), switching between them where necessary.

The switch between the torque estimator and the force estimator is practically instantaneous: all that is needed is to apply next equation (6):

$$F_{est} = \tau_{est} / l \quad (6)$$

Where  $\tau_{est}$  is equal to  $\tau_{newt}$  in the case of no interaction with the environment, or equal to  $\tau_{pres}$  if there is a collision.  $l$  is the distance between the rotation point and the tip of the arm on which the force is to be calculated.

## 5 HYBRID POSITION/FORCE CONTROL OF THE SET-UP

Figure 5 shows a diagram of the Hybrid Control implemented. It basically consists of a supervisor block that switches between position control and force control according to the status of the interaction between the arm and its environment (in this case, the lower limit stop). The position control is thus carried out separately from the force control, i.e. the system is controlled by the position algorithm until the supervisor block detects that a collision has occurred. When this happens, it switches between the controls as soft as possible, activating the force control.

### 5.1 Position Control Algorithm

The hybrid control structure enables different, independent algorithms to be implemented for position and force control. In the last few years the

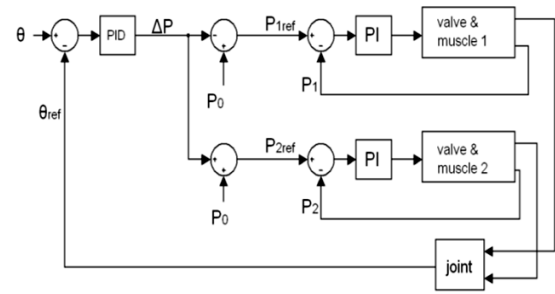


Figure 7: Diagram of the internal pressure loops based position control algorithm.

authors have conducted research into the position control of this same experimental device.

Owing to the fact that the results obtained with a classical PI controller were not good, due to its high non-linearity, other advanced control techniques were applied in order to correctly control the angular position. Firstly, a PID-based controller was enhanced with linear and non-linear internal loops. However, good performance requires the use of robust or non-linear control techniques (Thanh, 2006; Balasubramanian, 2007) and in this context, the application of different control techniques is found in the literature. Therefore, a robust linear control technique  $H_\infty$  (Pujana-Arrese, 2008), and a robust non-linear technique, sliding-mode (Arenas, 2008), were applied.

Subsequently, based on an idea applied by Tsagarakis and Caldwell (2007), a new position controller was developed based on an internal pressure loop for each muscle. This new position algorithm requires the use of one servo-valve for each pneumatic muscle instead of one single valve for each DoF, as used with the position algorithms that were designed and implemented previously.

Although this new solution initially doubles the variables that have to be controlled for each degree of freedom, it can be considered as a single-variable approach for each joint. Based on the symmetrical co-contraction of the opposing muscles, an asymmetrical variation is set in the pressure of each muscle. Thus, based on an initial pressure ( $P_0$ ) the setting is increased in one of the muscles and reduced by the same amount ( $\Delta P$ ) in the other.

$$P_{1ref} = P_0 - \Delta P; \quad P_{2ref} = P_0 + \Delta P \quad (7)$$

Accordingly, from the control point of view, the position control problem is still SISO with the angular position of the joint ( $\theta$ ) as the output and the pressure variation ( $\Delta P$ ) as the input.

Figure 7 shows the position control schematic based on the internal loops that control the pressure

Table 1: Force PID parameters for the different impact points.

	64.8°	48.2°	37.5	27.2°
$K_p$	0.045	0.025	0.03	0.025
$K_i$	0.05	0.05	0.03	0.04
$K_d$	0.002	0.0002	0.001	0.0005

in each muscle, implemented by means of PI algorithms. As it has been already mentioned, the pressure set-point for each controller is set on the basis of an initial value ( $P_0$ ), adding and subtracting the same quantity ( $\Delta P$ ). The value of this increase/reduction is the output of the most external loop of the controller (the position loop). This loop has also been implemented by means of a PID algorithm. The gains of both pressure loops were adjusted to the values  $K_p=4$ ,  $K_i=4$ , and the gains of the position loop to  $K_p=0.21$ ,  $K_i=1.2$ ,  $K_d=0.04$ , being  $P_0=3$  bar.

The experimental results for the hybrid position/force control shown later in this paper were obtained with the position algorithm based on the internal pressure loops tuned for a nominal load of 3 Kg placed at the tip.

## 5.2 Force Control Algorithm

Whereas direct measurement with the encoder located on the axis is the procedure used for position control, the value calculated by the force estimator is used to close the force control loop. The reaction of the device to any impact can thus be controlled without requiring the use of a sensor at the exact point of collision.

Unlike the case with position control, simulation-based tests confirm that to control the force correctly it is not necessary to design such complex algorithms. Also, the specifications of orthosis-type devices are much more restrictive for position control than they are for force control, in which it is normally sufficient for the force to be limited in the case of an inopportune collision.

The algorithm implemented is simply a PID tuned for a nominal load of 3 Kg. In any case, due to the non-linearity of the system, the response varies depending on the angular position in which switching between position control and force control occurs. With the aim of obtaining a more uniform response, four points distributed over the whole range of movement of the metal arm were selected.

These five points divide the movement of the system into five different zones. By means of impacts applied to these points, four different PID algorithms were tuned. Finally, a gain scheduling type strategy was implemented, which linearly combines the outputs of the two PIDs delimiting the zone in which the collision occurs.

Table 1 shows the PID algorithm parameter values for each of the points expressed according to their angular situation with respect to the vertical plane.

## 6 IMPEDANCE CONTROL OF THE SET-UP

The classic impedance control formulation is based on the hypothesis that the actuation system is able to supply the torque required by the control algorithm, i.e. the impedance control output is the torque set-point for the actuator. This hypothesis is not so evident in the case of one degree of freedom actuated by means of an antagonistic pair of pneumatic muscles. Tsagarakis (2007) puts forward the same algorithm based on the independent pressure loops used for controlling the angular position, which, as can be observed in Figure 7, is the one that has been implemented. As explained above, the scheme has two separate PI controllers for controlling the internal pressure of each muscle and an external loop governed by a PID, which in this case serves to close the torque loop. Logically, the tuning of the pressure loops is the same as in the case of the position control, i.e.  $K_p=4$ ,  $K_i=4$ , while the optimum values for the torque loop gains are  $K_p=0.12$ ,  $K_i=0.6$ ,  $K_d=0.0024$ .

The impedance control strictly speaking was implemented by adapting the general control law (1) to the experimental prototype presented in this study. The first step was to obtain a dynamic model of the system. In the field of robotics there are several methodologies for system modelling (including those of Newton-Euler and Lagrange-Euler), but in this case, given the mechanical simplicity of the prototype, the model was obtained by means of the physical equations.

First of all, the forces acting on the system needed to be identified. The intervening forces are the force of gravity and the two forces exerted by the pneumatic muscles. One of the muscles pulls upwards while the other pulls downwards. The resulting torque is the difference between them:



$$\sum \tau = I \cdot d\omega/dt \quad (8)$$

where  $I$  is the inertia of the body. When the existing forces had been established, the dynamic model was obtained by applying Newton's second law for the rotational movements:

$$\tau = -I \cdot d\omega/dt + m \cdot g \cdot L \cdot \sin \left[ \theta - \arctg \left( \frac{y_g}{x_g} \right) \right] \quad (9)$$

where  $m$  is the mass of the arm,  $\theta$  the angle between the vertical and the arm, and  $L$  the distance between the centre of gravity and the rotation point. Finally,  $x_g$  and  $y_g$  are the coordinates of the centre of gravity with respect to the rotation point.

To fully complete the dynamic model of the system, all that remains is to calculate the inertia  $I$ . The inertia of the arm with respect to its centre of gravity should be calculated (10), and transformed with respect to the rotation point by means of Steiner's theorem (11).

$$I_z = \frac{m}{12} \cdot (l^2 + a^2) \quad (10)$$

$$I_o = I_z + d^2 \cdot m^2 \quad (11)$$

where  $l$  is the length and  $a$  the width of the arm,  $d$  is the distance between the rotation point and the centre of gravity, and  $m$  the mass of the arm.

It has not been taken into account up to now that plates with extra weight can be placed on one end of the arm. To do this, the terms corresponding to the extra masses should be inserted in the dynamic model.

$$\begin{aligned} \tau = -I \cdot d\omega/dt + m \cdot g \cdot L \cdot \sin \left[ \theta - \arctg \left( \frac{y_g}{x_g} \right) \right] + N \\ \cdot m_p \cdot g \cdot L_p \cdot \sin \left[ \theta - \arctg \left( \frac{y_p}{x_p} \right) \right] \\ \cdot \sin \left[ \theta - \arctg \left( \frac{y_p}{x_p} \right) \right] \end{aligned} \quad (12)$$

where  $N$  is the number of extra masses,  $m_p$  the weight of each extra mass,  $L_p$  the distance between the centre of gravity of the extra weights and the rotation point of the arm, and  $x_p$  and  $y_p$  are the coordinates of the centre of gravity of the extra weights with respect to the rotation point.

The next step is to establish the reference impedance (13). In this case, the parameters  $K$ ,  $B$  and  $M$  are not matrixes but merely parameters simplifying the tuning process.

$$\tau_{int} + K(\theta_{ref} - \theta) + B(\omega_{ref} - \omega) = M \frac{d\omega}{dt} \quad (13)$$

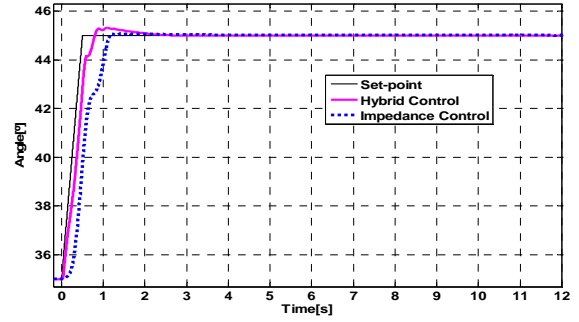


Figure 8: Experimental results in the intermediate displacement zone.

The impedance control law (14) to be applied, which is a simplified form of the general law (1), is obtained by equalling the term of the angular acceleration in (13).

$$\begin{aligned} \tau_{act} = -\frac{I}{M} \cdot K(\theta_{ref} - \theta) + S(\theta) - \frac{I}{M} \cdot B(\omega_{ref} - \omega) \\ - \frac{I}{M} \cdot \tau_{int} \end{aligned} \quad (14)$$

If the control law is analysed, apart from the parameters to be tuned ( $K$ ,  $B$  and  $M$ ), it can be observed that there is a term,  $\tau_{int}$ , which is the torque measured when the arm interacts with the environment. This torque can be the estimated torque, as described for the hybrid control, but it is not essential in the control law. This term was not used in the law implemented, as the results were analogous.  $S(\theta)$  represents the static part of the dynamic equation (12).

$$\begin{aligned} S(\theta) = m \cdot g \cdot L \cdot \sin \left[ \theta - \arctg \left( \frac{y_g}{x_g} \right) \right] + N \cdot m_p \cdot g \\ \cdot L_p \cdot \sin \left[ \theta - \arctg \left( \frac{y_p}{x_p} \right) \right] \end{aligned} \quad (15)$$

As can be observed, it is dependent on the mass at the tip, and it is therefore not robust to mass change. However, this mass can be estimated during the free movement phase. The design parameters  $K$ ,  $B$  and  $M$  were experimentally adjusted and the following values were obtained:  $K=3.1$ ,  $B=0$  and  $M=0.5$ .

To close the torque loop, the most common procedure is to use the direct reading by means of a torque sensor placed on the actual rotation axis, as done by Tsarakis (2007) and Jia-Fan (2008). However, as described in section 4 of this paper, an estimator was used to calculate the torque exerted by the antagonistic pair of muscles from the reading of their position and their internal pressures.



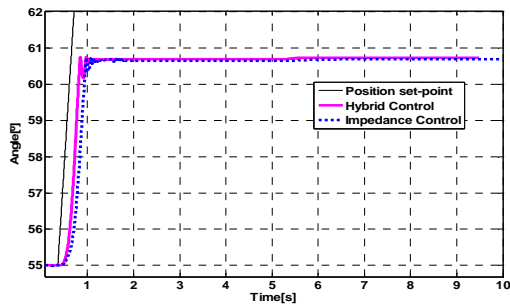


Figure 9: Position responses during a collision.

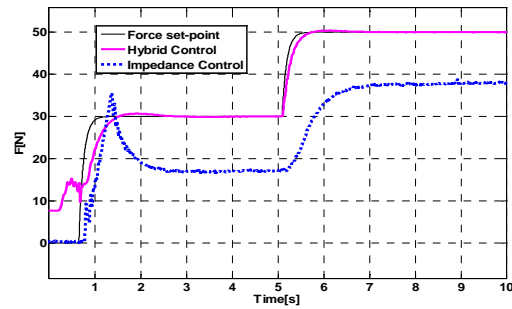


Figure 10: Estimated force responses during a collision.

## 7 EXPERIMENTAL RESULTS

Initially, controllers were tuned by simulation, using the non-linear model previously developed (Arrese-Pujana, 2007). Continuous-time controllers were discretized with sample time of 2 ms and then embedded into the control hardware.

With the objective of comparing the behaviour of both control techniques, Figure 8 shows the experimental response to a position step of  $10^\circ$  with a slope of  $20^\circ/s$ . This input signal has been applied to the intermediate zone within the motion range. Moreover, the arm has been loaded by attaching in its tip a weight of 3 Kg. This trial has been carried out in free movement without any collision with the environment.

The decoupling between the position and the force permits to adjust the hybrid control, thus it is possible to obtain a very fast position response which is almost identical in all the zones with a very little overshoot. Impedance control is not used to control explicitly the position, so, its response is more conservative because the same control law and the same tuning are used to control both the free movements and the collisions with the environment. Regarding the steady state error, both algorithms are able to eliminate it.

The trial showed in Figures 9 and 10 was performed in order to study the behaviour of both controllers with collisions. In this case, the arm is initially  $55^\circ$  away from the vertical plane and it is generated an ascendant position set-point with a slope of  $20^\circ/s$ . The lower limit stop was located at  $61.5^\circ$ , so when the arm tries to track the set-point and reaches this position a collision happens. Analyzing the dynamic of the position response (showed in Figure 9) it can be observed that the rebound happened after the collision has bigger amplitude with the hybrid control, due to the commutation between the position control and the force control. Fig 10 shows the estimate of the

force executed by the pneumatic muscles against the lower limit stop when the collision happens. In fact, during the collision, controllers are not comparable to each other. Hybrid control carries out the tracking of a force set-point whereas the reaction force of the impedance control is proportional to the error between the position set-point and the collision point. Force set-point for the hybrid control is 30 N for the first 5 s and then increases up to 50 N. After some initial disturbances due to the impact and the commutation between the controllers, the estimated force increases smoothly until it reaches the set-point. This response could be faster, but the parameters were tuned to achieve an acceptable force control with a weight placed in the tip within the range of 0 to 6 Kg. In the impedance control the influence of the collision is lower, and after an initial peak the estimated forced is limited. After the first 5 s position set-point increases, and the control reacts to this rise increasing the torque as it is shown in the graph of the force.

The robustness of the controllers can be tested by changes in the weight placed at the extreme of the arm. In Figure 11 it can be observed that the tuning performed for the hybrid controller is suitable to manage collisions with different loads within the range 0 to 6 Kg, although in the upper limit of the range (with 6 Kg) a minor overshoot happens. Hybrid control offers a robust behaviour in free movements as well.

Impedance control does not offer a robust behaviour with changes in the load. In fact, the algorithm (14) needs to specify the weight of the mass placed at the extreme of the arm. To solve this problem, it was developed an initialization function which it is used to carry out a set of free movements are useful to estimate the extra weight. Thus, the control systems can work autonomously. Once the extra weight is estimated the results showed in Figure 12 are obtained for different tip masses during a collision and maintaining the same control parameters.

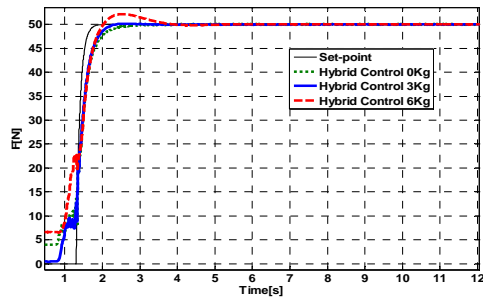


Figure 11: Estimated force response with different tip masses for hybrid control.

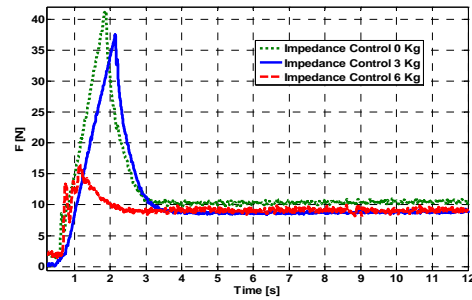


Figure 12: Estimated force response with different tip masses for impedance control.

## 8 CONCLUSIONS

This article is a study about the control issue of the interaction with the environment of a 1-DOF experimental set-up powered by pneumatic muscles. Due to the non linear behaviour of this kind of actuators the control of the mechatronic device is very complex both in free movements and when it comes into contact with an obstacle, having a different response depends on the movement zone or the position where the impact occurs. Moreover, the possibility of loading the extreme of the arm with extra weight requires using robust algorithms. The main contribution of this paper is the design and implementation of a torque/force estimator which is used to close the control loops. In spite of having a structural error derived from the equation used to model the force of the muscles, this inaccuracy only appears when the arm impacts with an obstacle and this is not critical because the dynamic is not affected.

## ACKNOWLEDGEMENTS

The material used in this paper was partly supported by the Spanish Ministry of Education and Science and European FEDER Fund (research project DPI2006-14928-C02-01).

## REFERENCES

- Thanh, T-D.C., Ahn, K.K., 2006. Nonlinear PID control to improve the control performance of 2 axes pneumatic artificial muscle manipulator using neural network. *In Mechatronics*, no. 16, pp. 577-587.
- Balasubramanian, K., Rattan, K.S., 2005. Trajectory tracking control of a pneumatic muscle system using fuzzy logic. *In NAFIP'2005, Annual Meeting of the North American Fuzzy Information Processing Society*.

- Pujana-Arrese, A., Riaño, S., Arenas, J., Martinez-Esnaola, A., Landaluze, J., 2008.  $H_\infty$  position Control of a 1-DoF Arm Powered by Pneumatic Muscles. *In the 8<sup>th</sup> Portuguese Conference on Automatic Control CONTROLO'2008*, 21-23 July 2008, Vila Real, Portugal.
- Arenas, J., Pujana-Arrese, A., Riaño, S., Martinez-Esnaola, A., Landaluze, J., 2008. Sliding-mode Position Control of a 1-DoF Set-up based on Pneumatic Muscles. *In UKACC Control Conference CONTROL2008*, 2-4 September 2008, Manchester.
- Tsagarakis, N.G., Caldwell, D.G., 2007. A compliant exoskeleton for multi-planar upper limb physiotherapy and training. *In ICAR'07, The International Conference on Advanced Robotics*, 21-24 August 2007, Jeju Island, Korea.
- Martinez, F., Retolaza, I., Lecue, E., Basurko, J., Landaluze, J., 2007. Preliminary design of an upper limb IAD (Intelligent Assist Device). *In the 9<sup>th</sup> European Conference for the Advancement of Assistive Technology, AAATE 2007*, October 3rd-5<sup>th</sup>, Donostia.
- Martinez, F., Retolaza, I., Pujana-Arrese, A., Cenitagoya, A., Basurko, J., Landaluze, J., 2008. Design of a Five Actuated DoF Upper Limb Exoskeleton Oriented to Workplace Help. 2008. *In IEEE International Conference on Biomedical Robotics and Biomechanics, IEEE BioRob 2008*, 19-22 October 2008, Scottsdale, Arizona, U.S.A..
- Pujana-Arrese, A., Arenas, J., Retolaza, I., Martinez-Esnaola, A., Landaluze, J., 2007. Modelling in Modelica of a pneumatic muscle: Application to model an experimental set-up. *In the 21<sup>st</sup> European Conference on Modelling and Simulation ECMS2007*, 4-6 June 2007, Prague.
- Raibert, M.H., Craig J.J., 1981. Hybrid Position/Force Control of Manipulators. *In Trans. of the ASME*, vol. 102.
- Hogan, N., 1985. Impedance Control: An Approach to Manipulation : Part I - Theory. Part II - Implementation. Part III - Applications. *In Journal of Dynamic Systems, Measurement, and Control*, 107, 1-24.
- Jia-Fan, Z., Can-Jun, Y., Ying, C., Yu, Z., Yi-Ming, D., 2008. Modeling and control of a curved pneumatic muscle actuator for wearable elbow exoskeleton. *In Mechatronics*, no. 18, pp. 448-457, 2008.